Published by :
http://www.ijert.org

International Journal of Engineering Research & Technology (IJERT)
ISSN: 2278-0181
Vol. 6 Issue 05, May - 2017

Sol-Gel Synthesized $CoFe_2O_4$ Nanoparticles: Structural and Magnetodielectric Properties

P. Divya[1], Y.Sreenidhi[1], T.Srihitha[1] and V. Niharika[1]
Department of EEE,
BVRIT Hyderabad College of Engineering for Women
Hyderabad, Telangana 500090

T. Ramesh[2*]
Department of Physics,
BVRIT Hyderabad College of Engineering for Women
Hyderabad, Telangana 500090

***Abstract*: Cobalt ferrite ($CoFe_2O_4$) nanoparticles have been successfully synthesized using the sol-gel auto-combustion technique. The structural properties of the synthesized powders were investigated using X-ray diffraction (XRD), Fourier transform infrared spectroscopy (FTIR). The examination of XRD patterns confirms the single-phase spinel structure, the crystallite size calculated by Scherer's formula is 17 nm. The FTIR spectra confirm the characteristic vibration of ferrite atoms at tetrahedral and octahedral sites, which confirm the spinel phase. The synthesized powders were densified using conventional sintering method at 850°C/3 hr. Structural and surface morphology of sintered sample was characterized using XRD and atomic force microscopy, respectively. The dielectric behavior as a function of frequency (100 Hz-1.8 GHz) was explained by Maxwell-Wagner two layer models and the Koop's phenomenological hypothesis. Magnetic properties such as coercivity, saturation, remanence, magnetic squareness, magneto crystalline anisotropy constant (K) and Bohr magneton were measured from the recorded M-H loops. Curie temperature was measured using gravity method. The optimized dielectric and magnetic parameters suggest that the $CoFe_2O_4$ material may be used for applications in magnetic resonance imaging and controlled drug delivery.**

Keywords: Ferrite, Sol-Gel, Magnetic properties, electrical properties.

I. INTRODUCTION

Nowadays, nanocrystalline ferrimagnetic (ferrite) materials are primarily studied in the search for improved properties and new applications due to their remarkable magnetic and electrical behavior [1-4]. Among various types of ferrimagnetic materials, cobalt ferrite ($CoFe_2O_4$) has been gained the great scientific attention of researchers positively because of its unique properties including large magneto crystalline anisotropy and magnetostrictive coefficient, moderate saturation magnetization, tunable coercivity, excellent mechanical hardness and stability [5-7]. As well as its exceptionally promising applications of magnetic resonance imaging (MRI), high-density magnetic recordings and medical diagnosis and treatment [8-11]. For these particular cases, however, an optimized magnetic and electrical properties are strongly required and these characteristics could be tuned by controlling the particle size and cation distribution in A and B-sites of ferrites, which in turn depends on the synthesis technique [12]. Traditional ceramic preparation methods for nano sized spinel ferrite often suffer from the uncontrolled stoichiometric poor composition, chemical inhomogeneity, contamination, coarser particle size and the introduction of impurities during ball milling/grinding and high annealing temperature. In addition, the coarse and non-uniform particles, on compacting, result in the formation of voids or low-density areas in the green compacts. Low-temperature chemical synthesis methods (co-precipitation, micellar route, sol-gel, hydrothermal, etc.) has overcome these drawbacks, produced ferrite nanoparticles with reproducible stoichiometric composition, and desired microstructures. In chemical methods, due to the mixing of chemicals at the molecular level, good chemical homogeneity with control on the shape and size distribution of nanoparticles can be achieved. Due to these reasons, the chemical methods of preparation have emerged as a very popular synthesis tool for nanoparticles of spinel ferrites.

In general, the chemical composition of a ferrite can be written as $A^{2+}B_2^{3+}O_4^{-2}$ which crystallize in the cubic crystal system with the oxide anions arranged in a cubic close-packed lattice and the cations A and B fully or partially occupy tetrahedral and octahedral sites [13]. The properties of ferrites strongly dependent on the distribution of cations amongst the available tetrahedral (A) and octahedral (B) sites. Therefore, the selection of composition and synthesis method plays a vital role in the preparation of ferrite nanoparticles with optimized properties. Hence, the focus of the present research is to improve the magneto-dielectric performance of cobalt ferrite. Hence, the cobalt ferrite nanoparticles were prepared using the sol-gel method and characterized by various analytical techniques to investigate the structural, morphological and the magneto dielectric properties. The obtained results have been examined and explained using different theories. The present study opens the window to understand the magneto electric behavior of cobalt ferrite, and hence, explore the technological applications.

II. MATERIALS AND METHODS

A. *Materials*

Cobalt ferrite nanoparticles were prepared by the sol-gel auto-combustion method. In this approach, Alfa Aesar AR grade cobalt nitrate hexahydrate (Co $(NO_3)_2.6H_2O$), iron (III) nitrate nano hydrate (Fe $(NO_3)_3.9H_2O$), and citric acid ($C_6H_8O_7.H_2O$) with purity 99.0% were used as starting materials without further purification.

B. *Synthesis*

The starting materials to prepare the cobalt ferrite nanoparticles were weighed according to the formula: Co $(NO_3)_2.6H_2O$+ Fe $(NO_3)_3.9H_2O$ ⇨ $CoFe_2O_4$. The stoichiometry amounts (1:2 =Co: Fe) of metal nitrates were dissolved in 200ml distilled water. The mixture was continuously stirred at room temperature using a magnetic stirrer until a dissolved solution is obtained. A required amount of citric acid, with

International Journal of Engineering Research & Technology (IJERT)
ISSN: 2278-0181
Vol. 6 Issue 05, May - 2017

citrate to nitrate ratio of 1.0, was added to the solution as chelating agent and fuel for the combustion process. Ammonia solution (25 %) was added to the precursor solution to adjust the pH of the solution. The solution was then heated up to 80°C using magnetic hotplate of the stirrer and becomes brownish gel after 15 min of stirring. Upon continues heating, the gel completely dried. It then swells, spontaneously combusted and burnt to form a dark greenish powder. The burned powder was then grounded and crushed using a mortar. The obtained fine powder was then calcined at 200°C for 120 min. Then the calcined powder was granulated using 2% PVA and then pressed into pellets at a pressure of 150MPa using the Hydraulic press. Pellet samples with about 10 mm diameter and 1.5 mm thickness were obtained and finally sintered at 850°C for three hours.

C. Characterization

PANalytical X'Pert Pro X-Ray Diffractometer characterized the phase structure behavior of as-prepared and sintered powders with Cu K_α radiation. A Fourier transform infrared spectrum (FTIR) of prepared particles was obtained using Brucker Tensor 7 spectrometer. The microstructure of investigated samples was studied using HITACHI S-4800 field emission scanning electron microscopy (FESEM). Frequency variation of electrical permittivity was measured in the frequency range of 100 Hz to 1.8 GHz using LCR (Zentech 3305) meter and impedance analyzer (Agilent 4291B). Magnetic properties such as saturation magnetization (M_S) remanence magnetization (M_r) and coercivity (H_C), were recorded at room temperature using vibrating sample magnetometer (VSM).

III. RESULTS AND DISCUSSION

X-ray diffraction (XRD) of $CoFe_2O_4$ reveals abundant information about the crystalline phase, lattice parameter, X-ray (theoretical) density, etc. of the prepared material. The obtained XRD peaks shown in Fig.1 are indexed using JCPDS card no. 22-1086. The sharp peaks concerning to the reflection planes (220), (311), (222), (400), (422), (511) and (440) in the XRD pattern confirm the formation of the cubic spinel structure. For the as-prepared powder, the XRD patterns represent the cubic phase which is the desired phase and also represent additional peaks of Fe_2O_3 (JCPDS card no. 89-8104) which is the undesired phase or appeared as a second phase and these second phase peaks disappear with further heat treatment. The lattice parameter (a), grain size (D_p), dislocation density (ρ_d), theoretical density (D_x), porosity (P) and strain (ε) are evaluated from the sintered X-ray diffraction results using the following relations [14] and the values are presented in Table 1.

$$a = d(h^2 + k^2 + l^2)^{1/2} \; ; D_p = 0.9\lambda/\beta \cos\theta \; ;$$

$$\rho_d = \left(D_p\right)^{-2}; \quad D_x = 8M/Na^3;$$

$$P = 1 - (D_b/D_x); \; \varepsilon = \beta/4 \tan\theta$$

Where d is the inter-planar spacing, (h k l) are the miller indices of the maximum intensity peak. λ is the wavelength of radiation used, β is the full-width half maximum of diffraction peaks, θ is the diffraction angle, M is the molecular weight of the ferrite, N is the Avogadro number and D_b is the bulk density measured using Archimedes principle.

Table.1 : Structural properties of sintered $CoFe_2O_4$

a(Å)	8.2702
D_P (nm)	40.61
ρ_d (m^{-2})	6.063×10^{-4}
D_x (g/cc)	5.905
D_b(g/cc)	5.542
P(%)	6.2
ε	0.0029

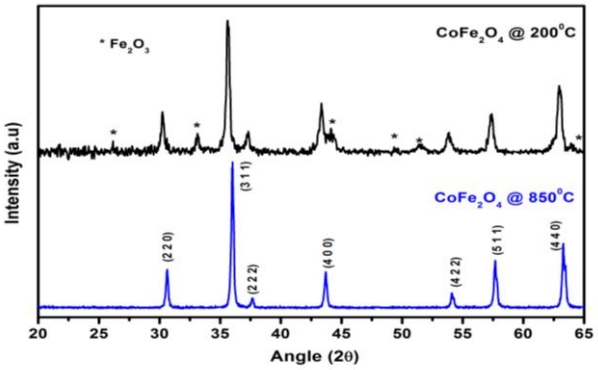

Fig.1 XRD patterns of synthesized and sintered $CoFe_2O_4$

FT-IR spectroscopy is a significant tool to investigate the stretching and bending vibrations of tetrahedral and octahedral complexes of ferrites. Fig.2 shows the IR absorption spectra of as prepared and sintered $CoFe_2O_4$ system.

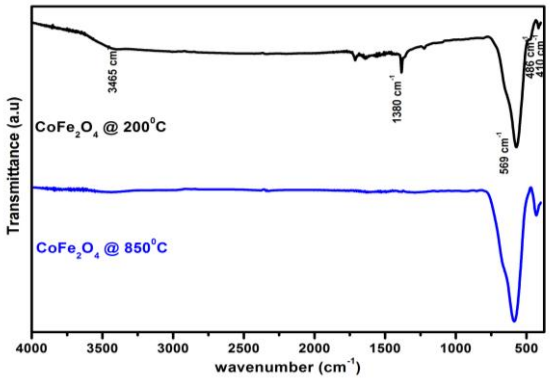

Fig.2 FTIR spectra of synthesized and sintered $CoFe_2O_4$

From the figure, it can be observed that the both powders shows two prominent absorption bands υ_1 and υ_2 in the range of 580 cm^{-1} and 410 cm^{-1} respectively. The absorption band 580 cm^{-1} (υ_1) corresponds to intrinsic stretching vibration of metal cations at the tetrahedral site, while the band 410 cm^{-1} (υ_2) corresponds to metal cations at the octahedral sites [15]. The difference in the band positions of ν_1 and ν_2 is because of the difference in the Fe^{3+}- O^{2-} distances for the octahedral and tetrahedral complexes [16]. These two absorption bands observed with in this limit reveal the formation of single-phase spinel structure having two sub-lattices, tetrahedral (A) site and octahedral [B] site. In addition, in the as prepared powders with the addition of characteristic bands, there is two more bands are observed at around 3400 cm^{-1} and 1600 cm^{-1} in as prepared powder represent the stretching and bending vibrations of H-O-H which indicates the presence of free or absorbed water.

International Journal of Engineering Research & Technology (IJERT)
ISSN: 2278-0181
Vol. 6 Issue 05, May - 2017

Atomic force microscopy (AFM) pattern of sintered $CoFe_2O_4$ sample is depicted in Fig. 3. It can be seen that the size of grains is uniform and in the nano regime. The micrographs show the presence of many interfaces. Figure 3 also shows the two-dimensional grain size distribution of the present samples. The present investigated sample show high density and most importantly, an entirely homogeneous microstructure. The chemical composition analysis of sintered sample is shown in Fig.4. The obtained results confirmed the expected stoichiometry without any trace of impurity.

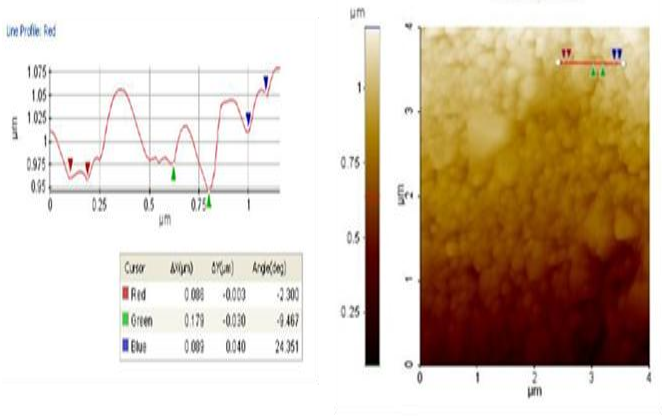

Fig.3 Atomic force microscopy (AFM) pattern of sintered $CoFe_2O_4$ sample

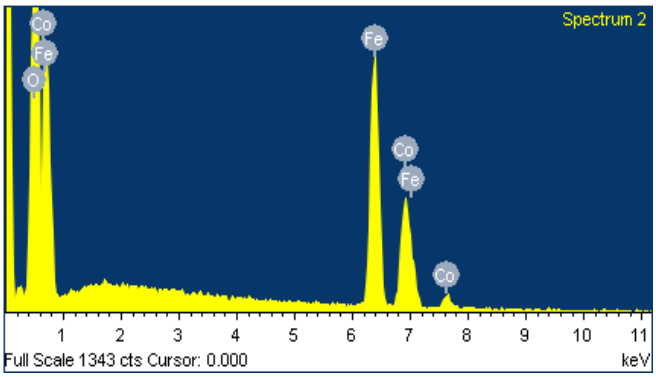

Fig.4 EDAX pattern of $CoFe_2O_4$ sample

In general, the dielectric constant (ε') gives information about the electrostatic energy stored per unit volume with per unit potential gradient. When it is used as a capacitor, it depicts the material capacity to store charge. Mathematically it is given as: $\varepsilon = \frac{Cd}{A\varepsilon_0}$; where, "C" is capacitance in farad, "d" is the pellet's thickness in meters, "A" is Area of cross section of the sample in square meters.

The Figs. 5 (a) and (b) shows the variation of real and complex part of the dielectric constant as a function of an applied ac field in the frequency ranges of 100 Hz to 1.8 GHz. It can be observed that the both the dielectric constant and complex dielectric constant decrease as the frequency increase from 100 Hz to 1.8 GHz. The decrease in dielectric constant relatively high at low frequency as compared to high frequency. The variation in dielectric constant can be understood by Maxwell-Wagner theory [17, 18] and Koop's model [19] by considering the ferrite system as a heterogeneous system with grains and grain boundaries possessing different conducting properties. In general, the fine conducting grains are separated by poorly conducting grain boundaries. The heterogeneous dielectric structure of the material is responsible for the space charge polarization. Hence, the dispersion occurring in the lower frequency regime is attributed to space charge polarization, since the electronic and atomic polarizations remain unchanged at these frequencies while at higher frequencies, the resonance peaks depend on the applied frequency and charge transfer frequency between Fe^{2+} and Fe^{3+} ions i.e. ionic relaxation. It can also be seen from the figure that there is one more dispersion is observed (around 1.2 GHz) is due to the Debye-type relaxation that is observed when the jumping frequency of the Fe^{2+} and Fe^{3+} ions matches the frequency of applied field [20]. Therefore, the dispersion at the low frequencies was due to space charge polarization effect and at higher frequency was due to the resonance of electrons.

The imaginary part of dielectric constant (Fig. 5(b)) follows the same trend with the increase in frequency as followed by the real part of dielectric constant and therefore, can be explained by using the Maxwell–Wagner model. The imaginary part of dielectric constant arises if the polarization lags behind the applied altering field and is caused due to the presence of impurities and structural inhomogeneities. The lower value of ε" obtained in the present sample can be attributed to the curtailing of the Fe^{2+} ions on account of the sol-gel process, resulting in better compositional stoichiometry and crystal structure. Moreover, it can also be seen that the drop in the imaginary part of the permittivity is more pronounced than the real part in the lower frequency region. The imaginary part of permittivity (ε') for the presently investigated samples is found to be low and remain constant in the broad frequency range of 100 kHz to 600 MHz. The lower value of ε" obtained in the present sample can be attributed to the curtailing of the Fe^{2+} ions on account of the sol-gel process, resulting in better compositional stoichiometry and crystal structure. The peak observed in the ε" at around 1.2 GHz, when the hopping frequency ($Fe^{2+} \Rightarrow Fe^{3+}$)of electrons becomes equal to the applied field frequency, where a maximum electrical energy is transferred to the oscillating ions and power loss shoots up, thereby resulting in resonance.

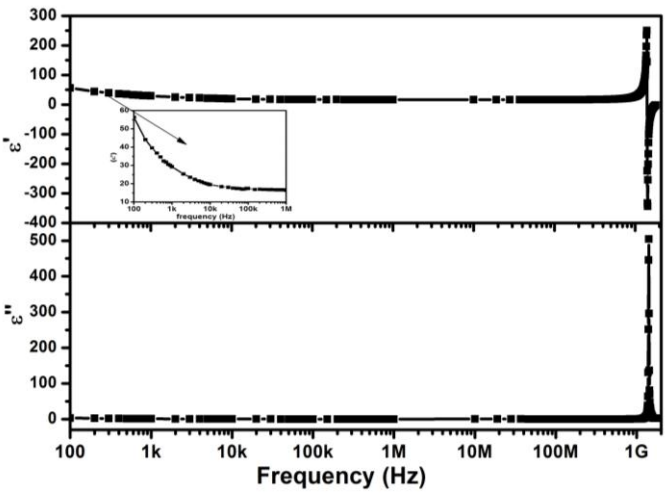

Fig. 5(a & b) Real and imaginary part of permittivity spectra of $CoFe_2O_4$ sample

International Journal of Engineering Research & Technology (IJERT)
ISSN: 2278-0181
Vol. 6 Issue 05, May - 2017

In general, the magnetization of ferrite material is a strong function of temperature, decreasing as temperature increases. This effect can be understood by noting that the vibrational energy of an atom increases with temperature, making it more difficult to align all the magnetic dipoles [21]. At high enough temperature the thermal energy is greater than the supplied by the internal magnetic field, and zero net magnetization results. This temperature is called the Curie temperature, T_C, where a ferrimagnetic to paramagnetic transition is observed. This principle was employed to determine the Curie temperature using gravity method. In this method, a small piece of ferrite sample is attached to the lower end of an iron rod and the upper end of which is placed vertically in contact with a pole piece of permanent electromagnet. The lower end of the iron rod along with the sample was enclosed in a furnace having a thermocouple for monitoring temperature. The temperature of the furnace is gradually increased till the ferrite sample losses its magnetization, falls due to gravity. The temperature at which the sample falls is taken as T_C. The value of T_C for the presently investigated sample is 765 K and it is well matched with the reported literature values.

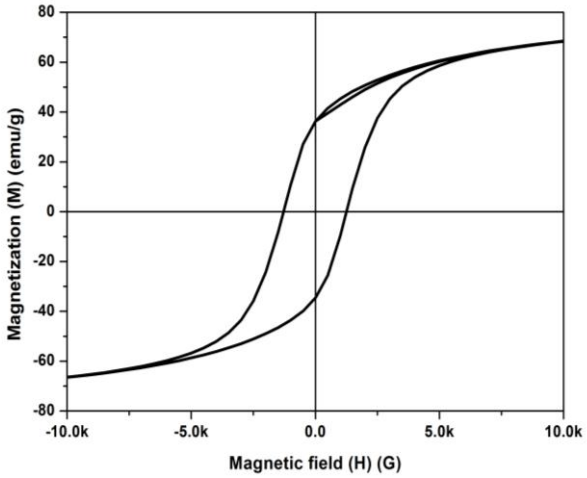

Fig.6 VSM pattern of $CoFe_2O_4$ sample

The room temperature magnetic properties of $CoFe_2O_4$ are investigated using vibrating sample magnetometer over the field range of ±10kOe as shown in Fig.6. It can be seen from the figure that the magnetization increases with increasing the applied magnetic field and attains saturation value at 0.4 T. The saturation magnetization (M_S), squareness factor (Mr/Ms), magnetic moment (μ_B), domain wall energy (ε_p) and critical diameter (D_C) are measured using the following equations (1) and (2) [22] and the obtained values are presented in Table 2. It is a known fact that the magnetic properties of ferrites are significantly affected by few extrinsic factors such as density, porosity and cationic distribution [23, 24]. The present investigated sample exhibited a saturation magnetization of 66.4 emu/g which is in agreement with other reports showing superior magnetic properties [24, 25]. The critical diameter (D_C) of a single domain is calculated using following formula:

$$D_C = \frac{1.4\varepsilon_p}{M_s^2} \dots\dots\dots (1)$$

Where $\varepsilon_p = (2k_bT_cK_1/a)^{1/2}$is domain wall energy, M_s is saturation magnetization in Gauss, K_b ($1.38*10^{-16}$ erg/K), T_C is Curie temperature in K, anisotropic constant $K_1 = H_C M_s/0.96$ in erg/cm^3 and 'a' is lattice parameter in cm [26].

$$\mu_B = \frac{M_W M_S}{5585} \dots\dots\dots (2)$$

Where M_W is the molecular weight of the stoichiometric composition and M_s is the saturation magnetization (emu/g).

Table 2 Dielectric and Magnetic properties of sintered $CoFe_2O_4$

ε' @ 100Hz	56.44
ε' @ 1MHz	16.37
ε" @ 100Hz	2.86
ε" @ 1MHz	0.03
Ms (emu/g)	66.40
Mr/Ms	0.55
μ_B	2.79
ε_p(erg/cm^2)	0.65
D_C(nm)	79
Hc (Oe)	2420
$K_1\times10^5$(erg/cm^3)	1.67
T_C (K)	765

IV. CONCLUSIONS

- The sol-gel synthesis method has been used to synthesize cobalt ferrite nanoparticles, consequently characterized, and then sintered at a temperature of 850°C for 3 h.
- The structural studies by XRD, morphology by AFM, magnetic measurements by VSM, magnetization as a function of temperature and dielectric measurements as a function of frequency at room temperature are performed and the results are discussed in detail.
- The examination of XRD patterns confirms the formation of single phase spinel structure with grain size 158 nm. The elemental analysis of the sample (EDAX) confirms the final stoichiometric. AFM micrograph confirms the grains are in nano meter regime and homogeneously distributed.
- Dielectric constant show dispersion in the low-frequency regime and remain constant after certain frequency limits confirm the frequency independent behavior. Dielectric loss factors of these samples also show a similar behavior on frequency.
- Magnetic hysteresis loop confirms the soft magnetic nature of sample with Ms and Hc is 66.40emu/g and 2420 Oe respectively.
- The saturation magnetization of material is a strong function of temperature, decreasing as temperature increases and the Curie temperature of the sample is 765 K.

ACKNOWLEDGMENT

The authors would like to thank Prof S.R.Murthy, Department of Physics, Osmania university for fruitful discussions. The authors are also very grateful to the Principal, BVRIT Hyderabad for her extensive support.

International Journal of Engineering Research & Technology (IJERT)
ISSN: 2278-0181
Vol. 6 Issue 05, May - 2017

REFERENCES

[1] R. Valenzuela, Novel applications of ferrites, Phys. Res. Int. 2012 (2012) 1–9.
[2] T. Ramesh, R.S.Shinde, S.R.Murthy, J.Magn.Magn.Mater. 345 (2013) 276-281.
[3] Goldman, A. Modern ferrite technology, 2nd ed.; Springer: Berlin, Germany, 2006; pp 217-226.
[4] R. Valenzuela, Magnetic Ceramics, Cambridge University Press, Cambridge, UK 1994.
[5] M.A. Ahmed, N.G.Imam, M.M Hefny, H.R.Gomaa, J. Ceram. Sci. Technol. 7(3), (2016) 235–241.
[6] A Pirouzfar, SA SeyyedEbrahimi, J MagnMagn Mater 370 (2014) 1–5
[7] Panpan Jing, JinluDu,ChendongJin, JianboWang,Lining Pan, JiananLi,Qingfang Liu, J. Mater. Sci. 51, (2016) 885–892.
[8] Fujun Liu, Sophie Laurent, Alain Roch, Luce Vander Elst, and Robert N. Muller,Journal of Nanomaterials, vol. 2013, Article ID 462540, (2013) 9 pages.
[9] D H Kim, D E Nikles, D T Johnson, C S Brazel, J Magn.Magn Mater 320 (2008) 2390–2396.
[10] Yunok Oh, MadhappanSanthaMoorthy, PanchanathanManivasagan, SubramaniyanBharathiraja, Junghwan Oh, Biochimie 133 (2017) 7-19.
[11] Farooq Ahmad and Ying Zhou, Chem. Res. Toxicol., 30 (2) (2017)492–507.
[12] S. Jauhar, J. Kaur, A. Goyal, S. Singhal, RSC Adv. **6**, (2016) 97694–97719.
[13] A. Goldman, "Crystal Structure of Ferrite," in Modern Ferrite Technology, 2nd ed., Springer, 2006, pp. 51-69.
[14] B.D. Cullity& S.R. Stock, Elements of X-Ray Diffraction, 3rdEd., Prentice-Hall Inc., 2001, pp. 167-171.
[15] R.D. Waldron, Phys. Rev. 99 (1955) 1727-1735.
[16] T.Ramesh and S. R. Murthy,Bull.Mater.Sci. 39(6), (2016) 1593-1601.
[17] J.C.Maxwell,Electricity and Magnetism, Oxford University Press, NewYork, 1973.
[18] K.W.Wagner,Am.Phys.40(1973)317.
[19] C.G. Koops,Phys.Rev.83(1951)121–124.
[20] Zaheer Abbas Gilani et al.,Physica E 73 (2015) 169–174.
[21] D.M. Pozar, Microwave Engineering, second ed., Wiley, Inc., New York, 1998.
[22] CosticaCaizer, Nanoparticle Size Effect on Some Magnetic Properties, Handbook of Nanoparticles, Springer International Publishing Switzerland 2015
[23] T. Ramesh, S. Bharadwaj, R. S. Shinde, S. R. Murthy ,AIP Conf. Proc. 1512, 408 (2013)
[24] Rabia Pandit, K.K. Sharma, Pawanpreet Kaur, R.K. Kotnala, Jyoti Shah, Ravi Kumar, J. Phys. Chem. Solids 75 (2014) 558–569.
[25] Souad Ammar et al., J. Mater. Chem., 2001, 11, 186-192.
[26] C. Caizer, M. Stefanescu, Nanocrystallite effect on σs and Hc in nanoparticles assemblies, Physica B 327 (2003) 129-134.